Journal of Materials Chemistry C

Accepted Manuscript

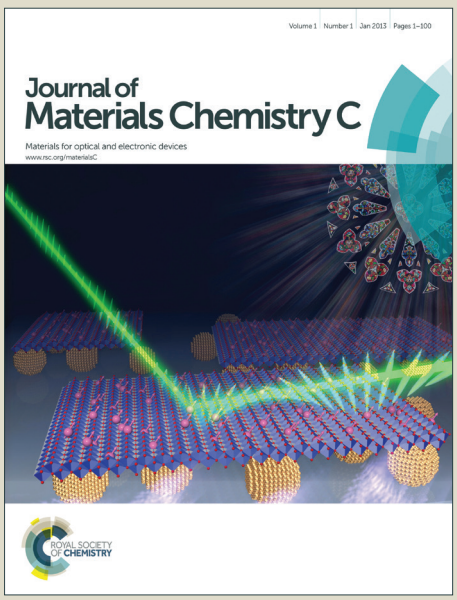

ROYAL SOCIETY OF CHEMISTRY

www.rsc.org/materialsC

Columnar Self-assembly of Star-shaped Luminescent Oxadiazole and Thiadiazole derivatives†

Suraj Kumar Pathak[#], Ravindra Kumar Gupta[#], Subrata Nath[#], Doddamane S. Shankar Rao[‡], S. Krishna Prasad[‡] and Ammathnadu S. Achalkumar*[, #]

[#]Department of Chemistry, Indian Institute of Technology Guwahati, Guwahati, 781039, Assam, India.
[‡]Centre for Nano and Soft Matter Sciences, Jalahalli, P. B. No. 1329, Bangalore, 560013, India.

†*Dedicated to Late Prof. S. Chandrasekhar*

KEYWORDS. 1,3,4-thiadiazole, 1,3,4-oxadiazole, Col_h phase, star-shaped molecule, Discotic liquid crystals

A new class of blue light emitting liquid crystalline star-shaped molecules based on 1,3,4-thiadiazoles have been designed and synthesized. These compounds were investigated by polarizing optical microscopy, differential scanning calorimetry, X-ray diffraction, cyclic voltammetry and photophysical studies. In comparison to their 1,3,4-oxadiazole counterparts, these thiadiazole based molecules are promising as they stabilize the hexagonal columnar phases over a broad thermal range. Thermal behavior and photophysical properties of these new star shaped molecules are extremely dependent on the number and types of peripheral tails in the molecular structure. 1,3,4-thiadiazole derivatives exhibit sky blue emission in solution in comparison to the deep blue emission of 1,3,4-Oxadiazole derivatives. They also exhibit lowered band gap in comparison to their oxadiazole counterparts and are promising for applications in organic light emitting diodes.

Introduction

Spontaneous self-assembly of shape anisotropic molecules into liquid crystalline (LC) phase/s is a subject that is attracting a great deal of curiosity in recent years. This unique combination of the order and fluidity in LC state is very important from the viewpoints of basic research as well as application.[1] Reinitzer's discovery of this phenomenon in cholesterol benzoate (calamitic/rod-like molecule) in 1888, arouse the curiosity of scientific community[2] and almost after a century, calamitic LCs became mainstay of display technology.[3] Discovery of discotic LCs (DLCs) by Chandrasekhar *et. al.*[4] in 1977 provided altogether a new dimension and the research in last four decades on DLCs is promising a bright potential in the area of organic electronics.[5] These disc like molecules either align with long range orientation to stabilize nematic (N) phase or stack one above the other to form columnar (Col) phase.[1] Discotic nematic materials have been used in the fabrication of optical compensation films for wide viewing angle liquid crystal displays (LCDs)[6] and also tested as active components in LCD devices.[7,8] Columnar phases formed from the strong overlap of central discotic cores with the insulating mantle of peripheral tails can act as molecular wires and may help in one-dimensional (1D) charge migration.[9] This property is of importance in the fabrication of optoelectronic devices like organic photovoltaic (OPV) cells,[10] organic light emitting diodes (OLEDs),[11] organic field effect transistors (OFETs)[12], gas sensors[13] and lubricants.[14]

The general design template of DLCs include the combination of a central rigid core connected to peripheral tails with the linking groups.[1,5] The central core is chosen in such a way that it can be either electron rich (*p*-type) or electron deficient (*n*-type) depending on the requirement. Recently there is a surge in the introduction of heterocylces in the molecular architecture due to the immense variety of the structures available and the tunability in the properties.[15] Presence of hetero atoms like N, O ans S in

the molecular structure impart reduced symmetry and a strong polar induction (lateral and/or longitudinal dipoles). When the electron deficient heterocylic rings are attached to aromatic rings, it leads to donor-acceptor interactions within the molecules. All these properties in turn affect the electronic and mesophase behavior. [15d] Hence mesogenic heterocyclic derivatives finding a strong foothold in the area of OLEDs as they provide a wide choice luminescence colors. They also enable polarized emission from oriented mesogens.[16] 1,3,4-Oxadiazoles are one such class of heterocycles, which are known for their advantageous features like hydrolytic, thermal stability and resistance to oxidative degradation. They are also known for their high fluorescence quantum yield and electron transporting properties. Because of these properties they are widely used as electron transporting/hole blocking and emissive layers in OLEDs.[15,17] Liquid crystalline oxdiazole derivatives have been extensively explored over the years. A vast number of 1,3,4-oxadiazole based calamitics,[18] discotics,[19] polycatenars,[20] V-shaped mesogens,[21a] supramolecular LCs,[21] ionic LCs,[22] bent core mesogens,[23] dimeric[24] and polymeric[25] mesogens have been reported. Besides the inherent advantages with oxadiazole based mesogens, there are certain drawbacks like high melting point, clearing point and narrow mesophase range which limits their applications.[26] 1,3,4-thiadiazoles are analogues of 1,3,4-oxadiazole derivatives where the oxygen atom is replaced with sulfur. This leads to very different properties to 1,3,4-thiadiazole derivatives, like higher melting and clearing temperatures, higher viscocity, efficient packing and larger dipole moments.[15c, 27] The larger atomic size of the sulfur in the case of hexahexylthiotriphenylene (HHTT), imparted an increased order in columnar packing and thus enhanced conductivity in comparison to hexaalkoxytriphenylene.[28] Compared to a large number of 1,3,4-oxadiazole based mesogens, reports on 1,3,4-thiadiazole based mesogens are scarce. This is partly due to the synthetic difficulty and low yields. Very few reports on calamitic mesogens,[29] banana mesogens[30] , hydrogen bonded LCs,[31] polymeric,[32] and polycatenars [26, 33] based on 1,3,4-thiadiazole are found in literature. Very recently there was a report on the synthesis of disk-like molecule bearing 1,3,4-thiadiazole unit stabilizing Col phase.

As part of our research program on the synthesis of luminescent LCs, we were interested to synthesize 1,3,4-oxadiazole and 1,3,4-thiadiazole based DLCs to understand their structure-property relationship. We wanted to optimize a simple route for the realization of hither to unreported 1,3,4-thiadiazole based DLCs. Since a common intermediate is used, we could prepare some of the 1,3,4-oxadiazole based DLCs. [19] In this paper we report the syntheses, characterization and thermal behavior of 1,3,4-oxadiazole and 1,3,4-thiadiazole based star shaped LCs (Fig. 1).

Results and discussion

Synthesis and Characterization. The synthetic route for the preparation of the target molecules and their precursors is depicted in scheme 1. General procedures for the syntheses of ethyl gallate, 3,4,5-trialkoxy ethyl gallates ethyl 3,4-dialkoxy benzoate are same as reported earlier.[35a] These alkoxy esters (**5a-d**) obtained by Williamson's protocol were converted to their respective hydrazides (**4a-d**) by treating with hydrazine hydrate in ethanol or *n*- butanol as solvent.[20k] Hydrazides **4a-d** were then refluxed with trimesic acid chloride in THF in presence of triethylaine to obtain tri-*N*-benzoylbenzohydrazides **3a-d**.[19a] Compounds **3a-d** were subjected to $POCl_3$ mediated dehydrocyclization to obtain trioxadiazoles **1a-d**.[19a] Similarly compounds **3a-d** on refluxing with Lawesson's reagent[35b] in toluene yielded corresponding trithiadiazoles **2a-d**.[31] Use of P_2S_5 did not provide good yield because of the incomplete reactions. The structures of all the intermediates and target molecules were confirmed using ^{1}H NMR, ^{13}C NMR, IR

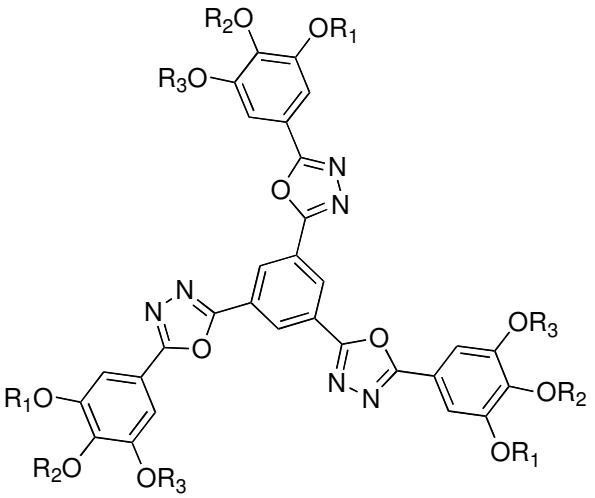

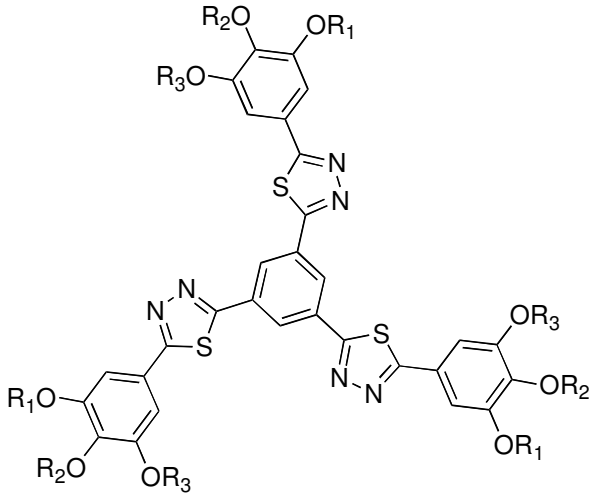

Figure 1. The molecular structures of star shaped 1,3,4-oxadiazole and 1,3,4-thiadiazole derivatives

Scheme 1. Synthesis of 1,3,4-oxadiazole and 1,3,4-thiadiazole based star shaped LCs.[a]

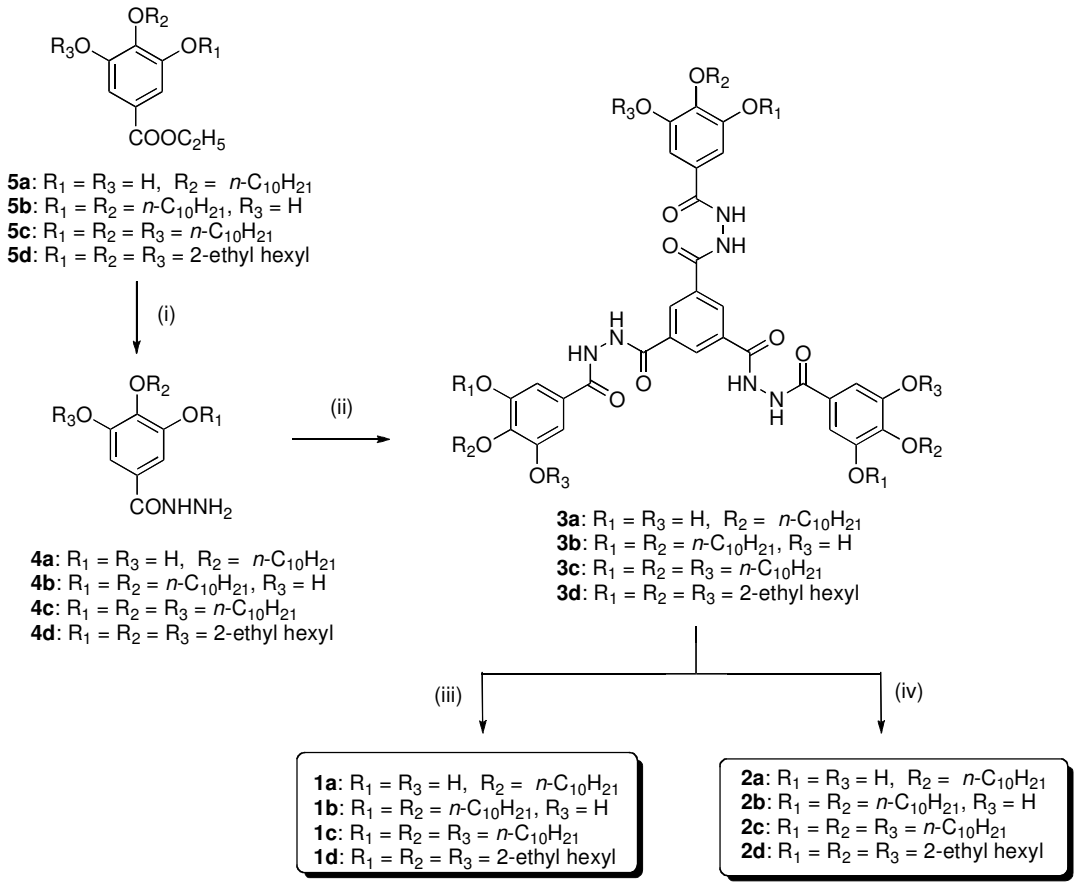

[a](i) $NH_2NH_2.H_2O$, Ethanol or butanol, reflux, 48 h (65-80%); (ii) Trimesic acid chloride, THF, Triethylamine, 6 h, reflux; (iii) $POCl_3$, reflux, 17 h (31-36%); (iv) Lawesson's reagent, toluene, reflux, 17 h (31-49%).

spectroscopy and ESI-HRMS or MALDI-TOF analysis. The ^{1}H NMR spectra of oxadiazole derivatives **1a-d** exhibited low field signals to aromatic hydrogens in comparison to their thiadiazole derivatives **2a-d**. The ^{13}C NMR of oxadiazole derivatives exhibited signals at δ values 166 ppm and 163 ppm for the carbons in heterocycle in comparison to the δ values 169 ppm and 166 ppm of the thiadiazole derivatives. (See the supporting information (SI) for the details).

Thermal behavior. All the compounds were investigated with the help of thermogravimetric analysis (TGA), Polarizing Optical Microscopy (POM) and Differential Scanning Calorimetry (DSC). Oxadiazole based compounds **1a-d** were stable at least upto ≈ 330 ^{o}C and complete degradation occurs at around 650 ^{o}C as evidenced by TGA. (See the SI). Phase transition temperatures and enthalpy changes obtained are presented in table 1. Oxadiazole based star shaped molecule **Ia** with three *n*-decyloxy tails,[19b] exhibited monotropic columnar hexagonal (Col_h) phase over a very short thermal range (4 degrees) with a grainy texture (see the SI). Compound **Ib** with six *n*-decyloxy tails showed an increased mesophase range (68 degrees) in comparison to **Ia**, with an isotropic temperature around 176 ^{o}C. On cooling the isotropic liquid dendritic texture develops which soon transforms into small pseudo focal conics and straight linear defects interspersed with homeotropic domains. This pattern is consistent with the texture for Col phases reported in literature.[36,5b] Around 84 ^{o}C, DSC thermogram showed a

Table 1. Phase transition temperatures [a] (^{o}C) and corresponding enthalpies (kJ/mol) of DLCs Col_h = Columnar hexagonal phase

	Heating	Cooling
1a	Cr_1 125.2 (13.8) Cr_2 137.6 (98.3) I	I 117.9 (27) Col_h [b] 113.1(69) Cr
1b	Cr_1 51.1 (92.7) Cr_2 83.4 (188.6) Cr_3 107.1 (266.9) Col_h 175.6 (18.4) I	I 174.5 (16.4) Col_h 83.7 (25) Cr_2 63.2 (14.2) Cr_1
1c	Cr 45.6 (86.2) Col 169 (15.5) I	I 168 (12.1) Col_{h1} 47 (71) Col_{h2} [c]
1d	Cr 111.8 (43.3) I	I 99.5 (38.6) Cr
2a	Cr_1 28 (10.7) $Cr_2$141.4 (81.8) Col_h 170.2 (80.3) I	I 166.1 (75) Col_h 122 (72) Cr
2b	Cr 93 (466.8) Col_h 155.3 (24.9) I	I 153.1 (18.1) Col_h [c] 65
2c	Cr_1 38 (24.1) Cr_2 48.8 (11.2) Col_h 206.1 (34.9) I	I 205.8 (28) Col_{h1} 46.6 (22.5) Col_{h2} [c]
2d	Cr 98.7 (49.8) Col_h 146.3 (15.8) I	I 140.8 (11.1) Col_h 84.2 (77.5) Cr

[a] Peak temperatures in the DSC thermograms obtained during the first heating and cooling cycles at 5 ^{o}C/min. [b] The phase observed is monotropic. [c] The mesophase is not crystallizing up to -20 ^{o}C

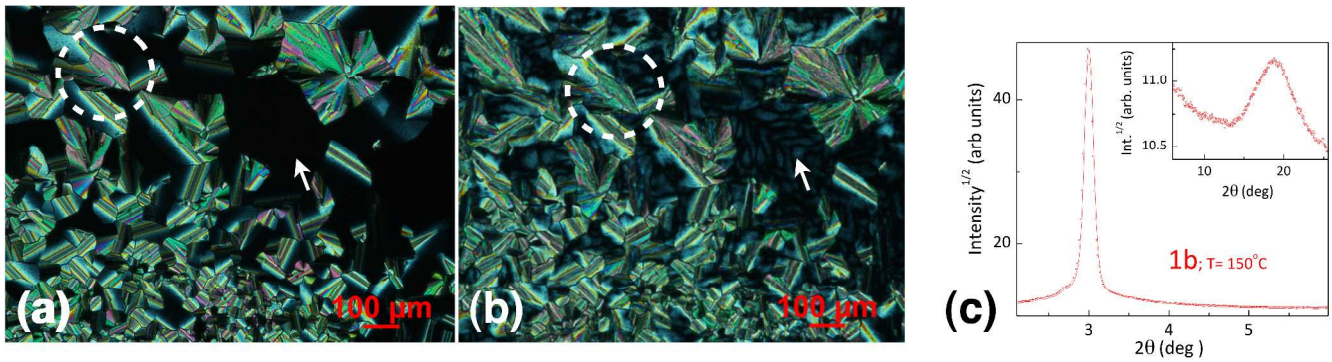

Figure 2. Photomicrographs of textures as seen by POM for the Col_h phase (a) at 154 °C and crystalline phase (b) at 74 °C of the compound **1b** (circled region and arrow shows the change in texture); (c) XRD profiles depicting the intensity against the 2θ obtained for the Col_h phase of compound **1b** at 150 ^{o}C.

mesophase-crystal transition with an enthalpy change of 25 kJ/mol, whereas the texture almost remained same but with a decrease in birefringence and fluidity. There were some changes in the color of pseudofocal conic fans and the appearance of defects in the homeotropic region (Figure 2a-b).

Powder XRD measurements were carried out to determine the symmetry of the thermodynamically stable Col phase formed by compound **1b** at temperature 150 ^{o}C. The results of indexing the sharp reflections of these profiles to lattice of Col phase are summarized in table 2.

Table 2. Results of (hkl) indexation of XRD profiles of the compounds at a given temperature (T) of mesophases[a]

Compounds (D/Å)	Phase (T/^{o}C)	d_{obs} (Å)	d_{cal} (Å)	Miller indices *hkl*	lattice parameters (Å), lattice area S (Å^2), molecular volume V (Å^3)
1b (47.68)	Col_h (150)	29.44 4.67 (h_a)	29.44	100	a = 33.99, S = 1000.9, V = 4674.5,[b] Z = 1.93[b]
1c (47.66)	Col_h (160)	28.64 4.63 (h_a)	28.64	100	a = 33.07, S = 947.3, V = 4384.3,[b] Z = 1.38[b]
	Col_h (100)	29.11 4.53 (h_a)	29.11	100	a = 33.61, S = 978.6, V = 4428.2,[b] Z = 1.39[b]
	Col_h (30)	29.97 4.43 (h_a)	29.97	100	a = 34.60, S = 1036.9, V = 4595.7,[b] Z = 1.44[b]

[a]The diameter (D) of the disk (estimated from Chem 3D Pro 8.0 molecular model software from Cambridge Soft). d_{obs}: spacing observed; d_{cal}: spacing calculated (deduced from the lattice parameters; a for Col_h phase). The spacings marked h_a and h_c correspond to diffuse reflections in the wide-angle region arising from correlations between the alkyl chains and core regions, respectively. Z indicates the number of molecules per columnar slice of thickness h_c, estimated from the lattice area S and the volume V. [b]In the absence of core-core peak, the spacings of the alkyl chain stacking (h_a) is taken for these calculations.

The X-ray profile of the Col phase showed (Figure 2c) a single strong reflection corresponding to a Bragg spacing d of 29.44 Å at the low-angle region, besides a diffuse peaks at about 4.64 Å in the wide angles. The presence of a single maximum at low angles precludes an explicit structural assignment; however, as often found in the literature,[35a, 37] such a pattern has been assigned to the Col phase been ascribed to a minimum in the form factor. The presence of a sharp peak in the low angle provides the distance between the adjacent (100) lattice planes d_{10}, from which the lattice parameter 'a' can be calculated. The intercolumnar distance for this phase was found to be 34 Å, which is substantially lower than the molecular diameter 47.7 Å. This may be due to the substantial free space available for the aliphatic chains. The diffuse halo found at 4.67 Å is typical of the liquid like order within the plane. Presence of this peak indicates that this is an ordered columnar hexagonal phase. To confirm whether the phase lying below 84 ^{o}C is crystalline or liquid crystalline/glassy state we have carried out XRD studies at 76 ^{o}C. The XRD profile showed several sharp reflections in the entire region ($2^{o}< 2\theta < 30°$) confirming that the phase in question is crystalline.

Compound **1c** with nine *n*-decyloxy tails showed an increment in the thermal range of mesophase (123 degrees), with a transition from crystal to mesophase at ≈ 46 ^{o}C with an enthalpy change of 86.2 kJ/mol and finally converting into an isotropic liquid at ≈ 169 ^{o}C. On cooling from the isotropic liquid,

it appears at 168 °C with the growth of small batonnets (Fig.3a). Further cooling results in the growth of these batonnets and their coalescence of anisotropic domains into a mosaic texture. This Col phase

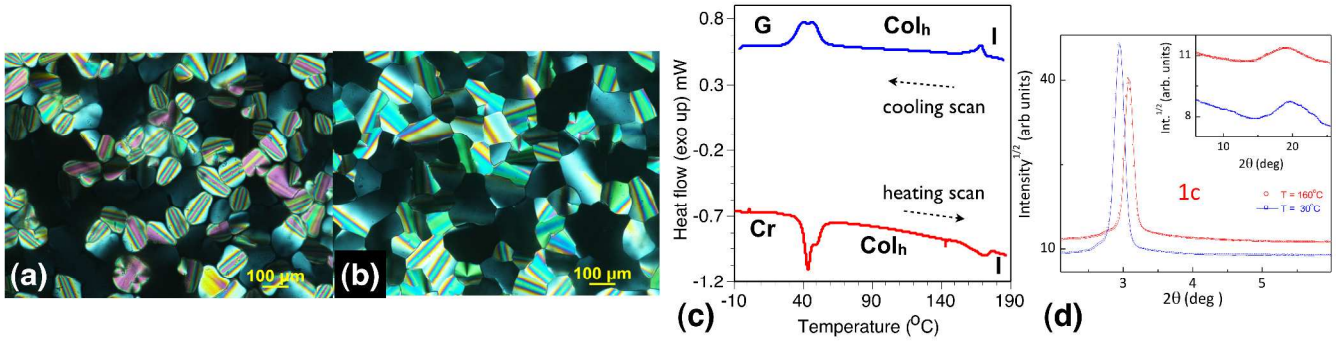

Figure 3. Photomicrographs of textures as seen by POM for the Col$_h$ phase of compound **1c** (a) at 152 °C and (b) at 30 °C; (c) DSC traces obtained for the first cooling (upper trace) and second heating (lower trace) cycles of **1c** at a rate of 5 °C min^{-1}; (d) XRD profiles depicting the intensity against the 2θ obtained for the Col$_h$ phase of compound **1c**

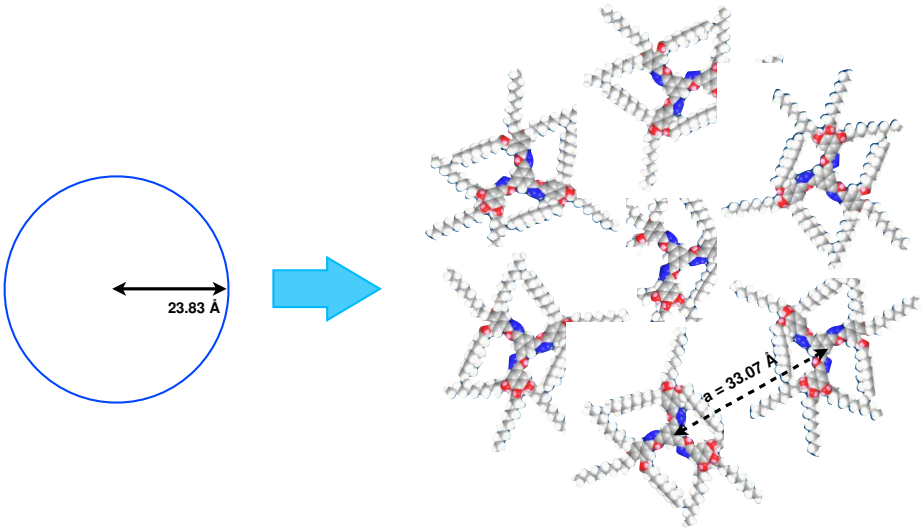

Figure 4. Schematic showing the self-organization of compound **1c** into hexagonal columnar (Col$_h$) lattice with inter-digitation of alkyl tails. Space filling energy minimized (all-trans) molecular model of **1c** derived from molecular mechanics (MM2) method.

persists till ≈ 47 °C undergoing a transition as evidenced by DSC with an enthalpy change of 71 kJ (Fig.3c). Even though this transition was observed in DSC, the texture remained same without a sign of crystallization (Fig.3b). Figure 3d indicates the 1D intensity versus 2θ XRD profiles obtained for the high (150 °C; blue trace) and low (30 °C; red trace) temperature Col phases of the compound **1c**. The patterns obtained at both temperatures were qualitatively similar with a sharp single peak at low angles and a diffuse maximum at wide angles. The spacings were however different with 28.64 Å and 4.63 Å at high-temperature, and 29.97 Å and 4.43 Å at low temperature. As discussed for the compound **1b**, we assign the Col$_h$ structure at both temperatures. A feature that differentiates the low temperature scenario from the high temperature one is the non shearability of the sample and unchanged optical texture of the

mesophase below 63 °C. In conjunction with the qualitatively same XRD pattern this suggests that the Col_h phase supercools into a glassy state. The marginal increase in the *d* value at low angle may be due

to the stretching of peripheral alkyl chains with a decrease in temperature. Again, the intercolumnar distance is substantially smaller than the molecular diameter (47.7 Å) estimated by the molecular model. While this could be due to the free space available for the chains as explained for the compound **1b**, it cannot fully explain the situation for the following reason. The diameter of the molecule estimated from the molecular model is the same for both **1b** and **1c**, but the intercolumnar distance is about 1 Å smaller for the later compound. Since the compound **1c** has more chains, the free volume available for each chain must be smaller than for compound **1b**. Thus, a possibility for the decreased spacing for **1c** could be intercalation of the peripheral alkyl tails into regions of the neighbouring molecule as shown in Fig.4.

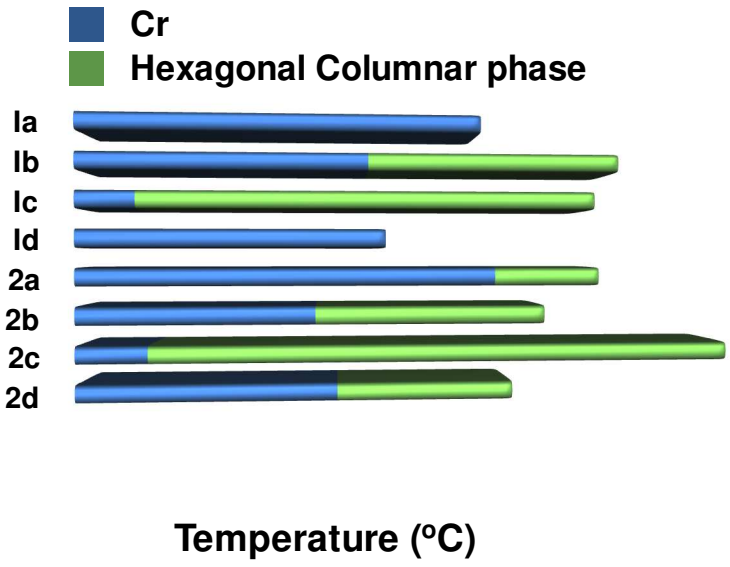

Figure 5. Bargraph summarizing the thermal behavior of compounds **1a-d** and **2a-d** (heating cycle)

In the case of compound **1d**, with nine branched tails we expected a huge decrease in melting point. This was expected due to the increased disorder at the periphery of these discotics due to the branching,[39] but surprisingly compound **1d** melted into an isotropic liquid at 112 °C without any LC phase. No mesophase was seen either in the cooling mode; instead the crystallization occurred with large fan like domains (Fig. S41). It is to be noted that similar oxadiazole derivative with six 2-ethylhexyloxy branched tails exhibited a Col_h phase.[19g] From these studies and as depicted in Fig. 5, it is evident that with the increase in the number of tails from **1a** to **1c**, the stability and range of the mesophase is increased (See Fig.5). Compound **1d** with the branched tails turned out to be crystalline; showing that introduction of branching in the periphery is not favorable in enhancing the mesophase range as in the case of conventional disc shaped LCs.[39]

The thermal stability of the thiadiazole derivatives **2a-d** were studied with the help of TGA under nitrogen atmosphere and found that all the compounds were stable at least upto ≈ 325 °C with complete degradation occuring at around 650 °C. (Fig. S51). Thiadiazole based star shaped molecule **2a** with three *n*-decyloxy tails showed an enantiotropic mesophase. This is significant when compared to the short-range monotropic behavior of **1a**. On heating the sample sandwiched between glass slides

exhibited a Cr-Cr transition at temperature of 28 °C and entered a mesophase at around 141 °C. The mesophase converted to isotropic liquid around 170 °C. The mesophase range of 30 degrees for compound **2a** is substantial when compared with its oxadiazole analogue **1a** with three alkoxy tails. On

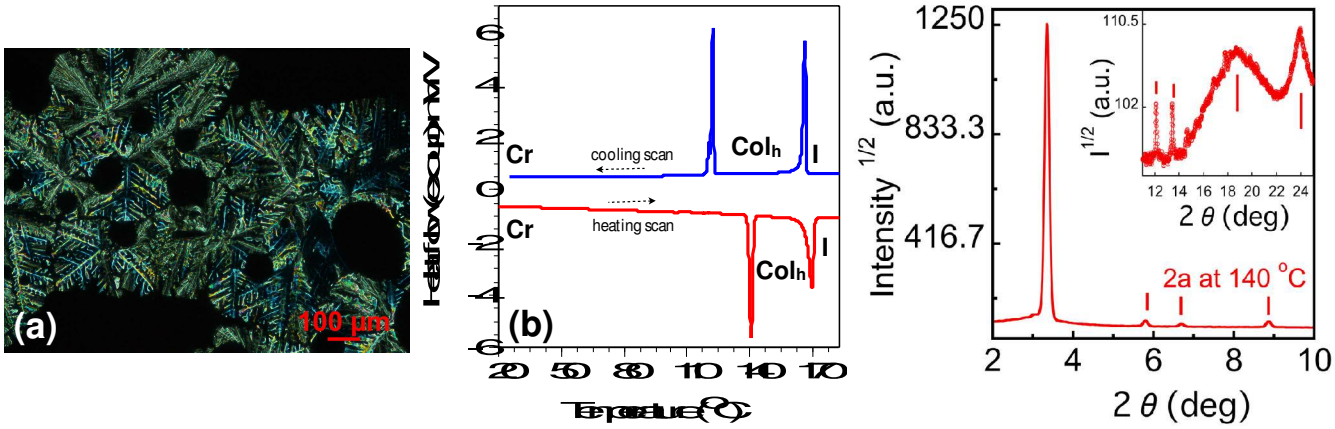

Figure 6. Photomicrograph of texture as seen by POM for the Col$_h$ phase at 163 °C (a); DSC traces obtained for the first cooling (upper trace) and second heating (lower trace) cycles of **2a** at a rate of 5 °C min^{-1} (b); XRD profiles depicting the intensity against 2θ obtained for the Col$_h$ phase of compound **2a** at 140 °C (c).

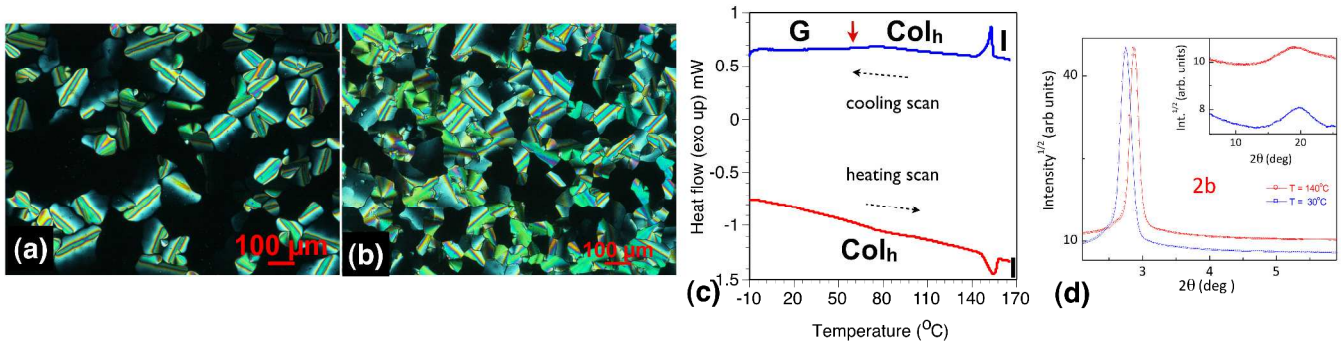

Figure 7. Photomicrographs of textures as seen by POM for the Col$_h$ phase (a) at 150 °C and (b) at 27 °C of the compound **2b**; (c) DSC traces obtained for the first cooling (upper trace) and second heating (lower trace) cycles of **2b** at a rate of 5 °C min^{-1}; (d) XRD profiles depicting the intensity against 2θ obtained for the Col$_h$ phase of compound **2b** at 140 °C and 30°C .

cooling the viscous isotropic liquid, a fern like texture developed which is consistent with the Col$_h$ phase (Fig.6a). Further cooling leads to the coales-cence of these pattern into a mosaic texture. The mesophase crystallized at 122 °C with an enthalpy change of 72 kJ/mol (Fig.6b). Thus it is evident that the presence of sulphur in the molecular structure is responsible for the enhanced mesophase range. The mesophase investigated with XRD studies at different temperatures confirmed that it is an hexagonal columnar phase (Table 2). XRD profile at 155 °C (SI) exhibited a sharp intense peak corresponding to *d* spacing of 26.4 Å along with other weaker peaks centered at smaller spacings in the ratio 1: 1/√3: 1/√4: 1/√7:1/3:1/√12. These values could be indexed to (100), (2-10), (200), (3-10), (310) and (400) reflections of the Col$_h$ mesophase. In the wide angles region two diffuse peaks are found at wide angle at 4.69 Å and 3.79Å, the feature becoming clearer at low temperature (Fig. 6c). The first one is due to the packing of alkyl tails, while the second one corresponds to stacking of the molecular cores within

the column. The latter being stronger than the former indicates that the discs are well ordered within the column.

Thiadiazole derivative **2b** with six *n*-decyloxy tails, exhibited a Col mesophase over a broad range from 93 °C to 155 °C in heating cycle. On cooling the isotropic liquid, the mesophase appeared in the

Table 3. Results of indexation of XRD profiles of compounds at a given temperature (T) of mesophases

Compounds (*D*/Å)	Phase (T/°C)	d_{obs} (Å)	d_{cal} (Å)	Miller indices *hkl*	Lattice parameter (Å), lattice area S (Å²), molecular volume V (Å³)	(hkl) of the
2a (48.45)	Col_h (155)	26.40	26.42	100	*a* = 30.51; S = 806.2; V = 3058.2; Z = 1.79	
		15.27	15.26	2-10		
		13.23	13.21	200		
		9.99	9.99	3-10		
		7.33	7.33	310		
		6.61	6.61	400		
		4.69 (h_a)				
	Col_h (140)	3.79 (h_c)	26.37	100		
		26.36	15.22	2-10	*a* = 30.45; S = 803.0; V = 2985.3; Z = 1.75	
		15.23	13.19	200		
		13.20	9.97	3-10		
		9.97	7.31	4-30		
		7.32	6.59	400		
		6.60				
		4.74 (h_a)				
		3.72 (h_c)				
2b (48.43)	Col_h (140)	30.72	30.72	100	*a* =35.47; S = 1089.7; V = 5058.2;[b] Z = 2.04[b]	
		4.64 (h_a)				
	Col_h (100)	31.44	100		*a* = 36.3; S = 1141.3; V = 5242.1;[b] Z = 2.1[b]	
		31.40	18.15	2-10		
		18.13	15.72	200		
		15.84				
	Col_h (30)	4.59 (h_a)	32.12	100	*a* = 37.09; S = 1191.3; V = 5306.7;[b] Z = 2.14[b]	
		32.12				
		4.45 (h_a)				
2c (48.42)	Col_h (190)	29.35	29.35	100	*a* = 33.89; S = 994.8; V = 4138.8;[b] Z = 1.27[b]	
		4.16 (h_a)				
	Col_h (130)	29.73	29.73	100	*a* = 34.33; S = 1020.8; V = 4323.5;[b] Z= 1.33[b]	
		4.24 (h_a)				
	Col_h (30)		31.8	100	*a* = 36.72; S = 1168.0; V = 4951.6;[b] Z = 1.52[b]	
		31.80				
		4.24 (h_a)				
2d (37.99)	Col_h (180)	26.03	26.03	100	*a* = 30.06; S = 782.5; V = 3034.3; Z = 1.07	
		4.63 (h_a)				
	Col_h (108)	3.88 (h_c)	26.0	100	*a* = 30.02; S = 780.3; V = 3086.4; Z = 1.09	
		26				
		4.54 (h_a)				
		3.96 (h_c)				

[a]The diameter (D) of the disk (estimated from Chem 3D Pro 8.0 molecular model software from Cambridge Soft). d_{obs}: spacing observed; d_{cal}: spacing calculated (deduced from the lattice parameters; *a* for Col_h phase). The spacings marked h_a and h_c correspond to diffuse reflections in the wide-angle region arising from correlations between the alkyl chains and

core regions, respectively. Z indicates the number of molecules per columnar slice of thickness h_c, estimated from the lattice area S and the volume V. [b]In the absence of core-core peak, the spacings of the alkyl chain stacking (h_a) is taken for these calculations.

form of small batonnets (Fig. 7a), which have grown in size and finally coalesced. The mesophase did not show any signs of crystallization even at room temperature as observed under POM (Fig.7b). No signs of crystallization were observed in the DSC scan even up to a temperature of -20 ^{o}C, thus confirming the frozen Col structure. (Fig.7c) The XRD profile confirmed he- -xagonal columnar structure right down to room temperature. Though these two profiles depicted a single peak at low angles, the XRD pattern obtained at 100 ^{o}C showed more reflections at higher angles fitting into a Col_h lattice. However, reflection at wide angles corresponding to core-core stacking was not observed indicating loose packing of the discs within the column (Fig. 7d and Table 3).

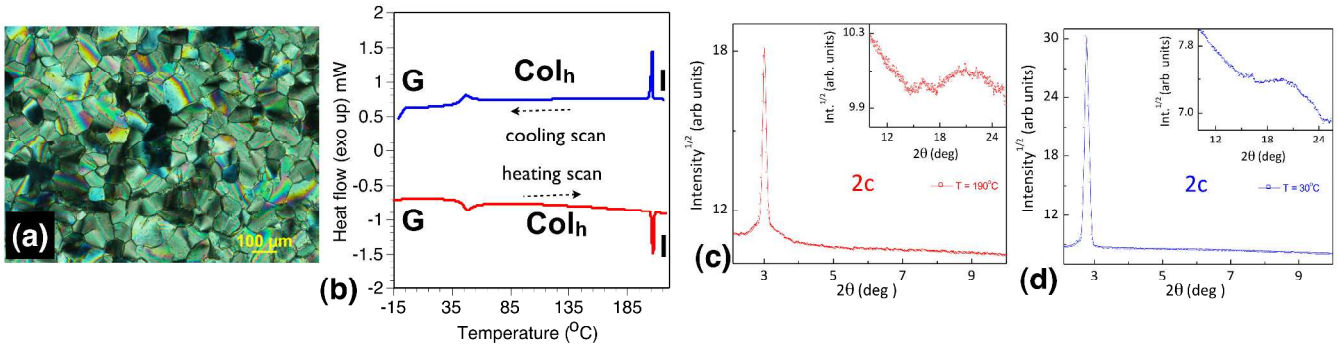

Figure 8. Photomicrographs of textures as seen by POM for the Col_h phase (a) at 30 °C; (b) DSC traces obtained for the first cooling and second heating cycles of **2c** at a rate of 5 °C min^{-1}; The intensity *vs* 2θ profiles extracted from the XRD patterns of the Col_h phase (c) at 190 ^{o}C and (d) at 30 ^{o}C for compound **2c**.

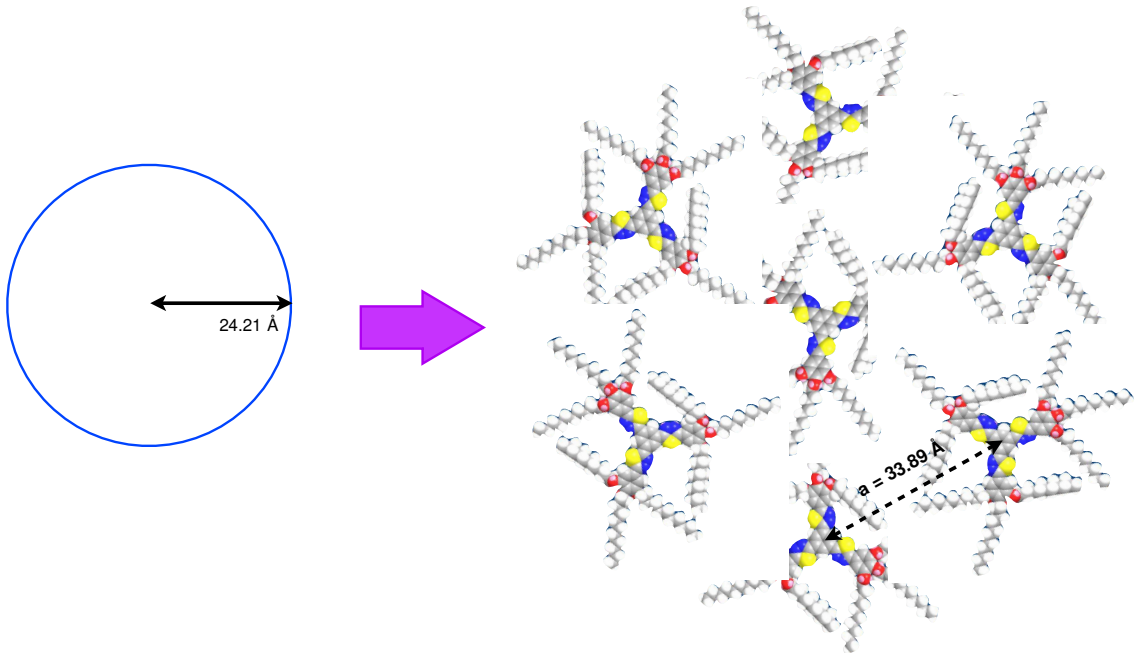

Figure 9. Self-organization of compound **2c** in hexagonal columnar (Col_h) lattice. Space filling energy minimized (all-trans) molecular model of **2c** derived from molecular mechanics (MM2) method.

Compound **2c** with nine *n*-decyloxy tails exhibited an increased thermal range for Col phase from 49 ^{o}C to 206 ^{o}C. On cooling from the isotropic liquid the mesophase appeared with a mosaic texture specific to Col phase which remain unchanged at room temperature (Fig.8a). In DSC scan there was a phase transition around 47 ^{o}C with an enthalpy change of 22.5 kJ/mol (Fig.8b), but no change in the optical texture. The nonshearability of the compound with the unchanged texture confirmed the glassy nature of the structure. X-ray diffraction studies carried out at 190 ^{o}C showed the mesophase is columnar with D_{6h} symmetry with an intercolumanr distance of 33.9 Å. Similar pattern was observed for XRD carried out at 130 ^{o}C and 30 ^{o}C showing that the Col_h phase is of broad thermal range freezing into a glassy state at low temperatures. This feature is favorable for charge migration with concomitant freezing of ionic impurities.[38] The molecular packing could be again of the intercalating type shown in Fig. 9

Compound **2d** with nine branched tails did not show any abrupt decrease in melting point as expected, but exhibited a hexagonal columnar mesophase over a thermal range of 48 degrees as confir - med by POM, DSC and XRD studies. This behavior is in con trast to its oxadiazole counterpart **1d**. These studies on com-pounds **2a-d** again showed the same trend as in the case of oxadiazole derivatives (**1a-d**) (Fig. 5). The mesophase range increases with number of tails while branching in the peripheral tails the opposite effect as observed in the case of **2d**. Overall, the thiadiazole derivatives exhibit enhanced mesophase range in comparison to oxadiazole derivatives. This is more evident in the case of compound **2a** with a mesophase range of 31 degrees; in comparis-on to monotropic compound **1a**. Similarly the enhanced mesophase range of compound **2d** with respect to crystalline compound **1d** is an example, reiterating the propensity of thiadiazole ring in improving the thermal behavior. We can assign this enhancement solely to the presence of thiadiazole moiety.

Photophysical properties. Photphysical properties of these star shaped molecules in solution are depicted in table 4. Absorption and fluorescence spectra of the compounds **1a-d** and **2a-d** were taken in micromolar solutions in THF. As can be seen, the absorption spectra obtained for the solutions of **1a-d** showed a single absorption maximum in a range of 312-324 nm, while the absorption spectra of **2a-d** showed a bathochromic shift. The absorption maximum of compounds **2a-d**, were centered at around 335-350 nm. Both the series of molecules showed large values of molar absorption coefficients showing that these are highly conjugated systems (ε = >25,000 M^{-1} cm^{-1}). Based on the similarity to previous 1,3,4-oxadiazole based systems, the single absorption band of these systems is attributed to spin allowed π- π^* transition of the aromatic system.

Emission spectra of compounds **1a-d** obtained by exciting the solutions of these compounds at their absorption maxima showed emission with their maxima centered around 388-458 nm (Fig. 10a). It is surprising to see that compound **1b** with six alkyl tails showed a large shift in the emission maximum with an emission maximum at 434 nm with a large Stoke's shift of 110 nm. Such large shift in the emission maximum accounts for the large delocalization of electron cloud when compared to compound **1a**. Compound **1c** exhibited an emission maximum centered at 461 nm with a Stoke's shift of 143 nm. Compound **1d** was similar to **1c**, except the alkoxy tails were branched. As expected the compound **1d** exhibited an emission maximum (458 nm, Stoke's shift 139 nm), which did not differ much from **1c**. This shows that number of alkoxy tails on the aromatic moiety have significant effect on the emission properties than the nature of the alkoxy tails. Emission spectra of compounds **2a-d** obtained by exciting

them at their absorption maxima showed an emission maxima centered around 416-471 nm (Fig. 10b). Similar to compounds **1a-d**, we observed a bathochromic shift in the emission with the increase in the number of tails as we move from **2a** to **2c**, while the emission of compound **2d** did not differ much from com pound **2c**. The observed red shift in absorption and emission of thiadiazole derivatives is due to the higher polarizability and basic nature of sulphur in the thiadiazole moiety. Quantum yields of these

Entry	Absorption (nm)	Emission[c] (nm)	Stokes shift nm (cm^{-1})	Quantum Yield[i]	λ_{onset} (nm)	$\Delta E^{d,e}_{g,opt}$	E^{f}_{1red}	$E^{d,g}_{HOMO}$	$E^{d,h}_{LUMO}$
1a	312	388	76 (6378)	0.45	357	3.48	-1.24	-6.52	-3.04
1b	324	434	110 (7822)	0.43	371	3.35	-1.13	-6.50	-3.15
1c	318	461	143 (9755)	0.48	370	3.36	-1.34	-6.3	-2.94
1d	319	458	139 (9514)	0.47	369	3.37	-1.45	-6.2	-2.83
2a	335	416	81 (5812)	0.25	383	3.24	-1.27	-6.19	-2.95
2b	350	447	97 (6200)	0.29	403	3.08	-1.21	-6.15	-3.07
2c	345	471	126 (7755)	0.31	398	3.12	-1.07	-6.33	-3.21
2d	345	470	125 (7709)	0.26	400	3.11	-1.25	-6.14	-3.03

Table 4. Photophysical[a] and electrochemical[a,b] properties of star shaped molecules

[a]micromolar solutions in THF; [b] the excited at the respective absorption maxima; [c] Experimental conditions: $Ag/AgNO_3$ as reference electrode, Glassy carbon working electrode, Platinum rod counter electrode, TBAP (0.1 M) as a supporting electrolyte, room temperature, [d] In electron volts (eV), [e] Band gap determined from the red edge of the longest wave length in the UV-vis absorption spectra, [f] In volts (V), [g] Estimated from the formula $E_{HOMO} = E_{LUMO} - E_{g,\ opt,}$ [h]Estimated from the onset reduction peak values by using $E_{LUMO} = -(4.8 - E_{1/2,\ Fc,Fc^+} + E_{red,\ onset})$ eV. [i] Relative quantum yield calculated with respect to quinine sulphate solution in 0.1 M H_2SO_4 with a quantum yield of 0.54.

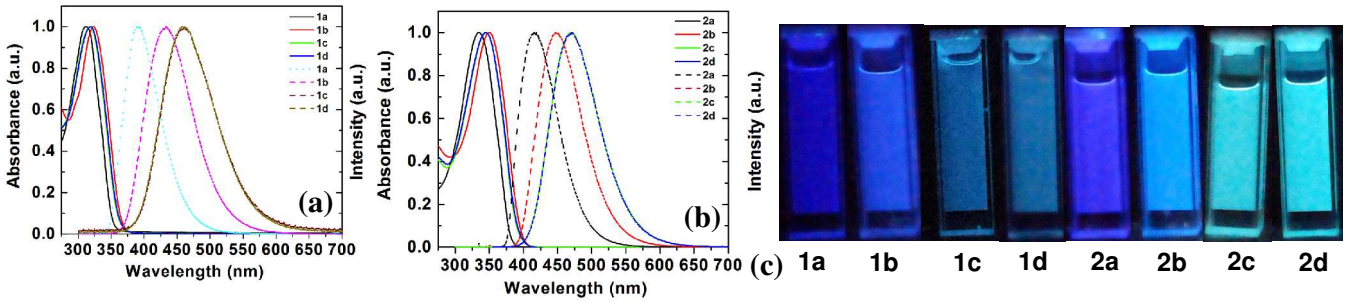

Figure 10. Normalized absorption (solid line) and emission spectra (dotted line) in THF solution obtained for **1a-d** (a) and **2a-d** (b) Pictures of micromolar solutions of compounds **1a-d** and **2a-d** in THF as seen with the illumination of 365 nm light (c)

compounds were measured with respect to Quinine sulphate solution (in 0.1 M H_2SO_4 with quantum yield of 0.54). Oxadiazole based compounds **1a-d** showed quantum yields in the range 0.43 to 0.48, whereas thiadiazole based compounds showed slightly lesser quantum yields ranging from 0.25 to 0.31. As can be seen in the Fig.10c, blue light is visually perceivable in the emissive state for both the series of compounds. Oxadiazole derivatives exhibited deep blue emission while thiadiazole derivatives exhibited sky blue emission. This is promising as the blue light emitting materials are not only limited but also their energy levels are high. They provide an efficient approach in fine-tuning the emission wavelength on combining with another dopant emitter in the construction of white OLEDs.[40]

Electrochemical properties. Cyclic voltammetry (CV) gives valuable information and allows the estimation of HOMO and LUMO levels of the organic materials. All the star shaped molecules were investigated for their electrochemical behavior by carrying out cyclic voltammetry studies in anhydrous micromolar THF solution. The energy levels and band gaps calculated from these studies are tabulated in table 4. A 0.1 M solution of tetrabutylammonium perchlorate (TBAP) was used as a supporting electrolyte in deoxygenated THF. A single compartment cell equipped with $Ag/AgNO_{3\ (0.1M)}$ reference electrode, platinum rod counter electrode and glassy carbon working electrode was used for the experiments. The reference electrode was calibrated with the ferrocene/ferrocenium (Fc/Fc^{+}) redox couple (absolute energy level of –4.80 eV to vacuum).[41] The cyclic voltammograms were recorded with a scanning rate of 0.05 mVs^{-1}. All the compounds exhibited well-defined irreversible oxidation and reduction waves (See SI). The optical band gap $E_{g,opt}$ was estimated from the red edge of the absorption spectra.

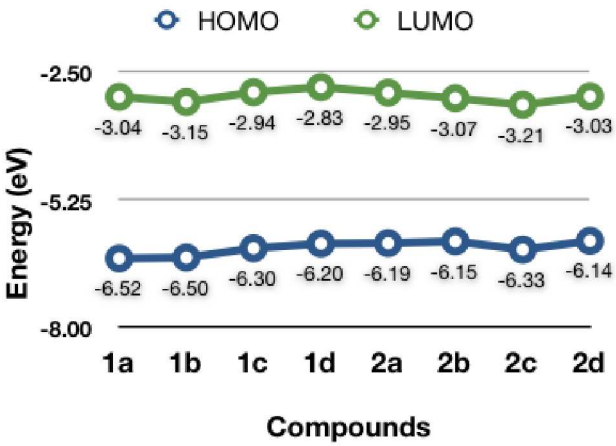

Figure 11. The HOMO and LUMO energy levels obtained for compounds **1a-d** and **2a-d**.

Oxadiazole derivatives **1a-d** exhibited higher band gaps when compared to thiadiazoles **2a-d** (Table 4). Energy levels LUMO were determined by using the formula $E_{LUMO} = -(4.8 - E_{1/2,\ Fc,Fc^{+}} + E_{red\ onset})$ eV, while HOMO energy levels were determined by using the formula $E_{HOMO} = E_{LUMO} - E_{g,\ opt.}$ Oxadiazole based compounds **1a-d** exhibited LUMO levels -3.04 eV, -3.15 eV, -2.94 eV and -2.83 eV, while thiadiazole based compounds **2a-d** exhibited LUMO levels -2.95 eV, -3.07 eV, -3.21 eV and -3.03 eV respectively (Fig. 11 and Fig. S49).

Experimental Section

Commercially available chemicals were used without any purification; solvents were dried following the standard procedures. Chromatography was performed using either silica gel (60-120 and 100-200) or neutral aluminium oxide. For thin layer chromatography, aluminium sheets pre-coated with silica gel were employed. IR spectra were recorded on a Perkin Elmer IR spectrometer at normal temperature by using KBr pellet. The spectral positions are given in wave number (cm^{-1}) unit. NMR spectra were recorded using Varian Mercury 400 MHz or Bruker 600 MHz NMR spectrometer (at 298K). For ^{1}H NMR spectra, the chemical shifts are reported in ppm relative to TMS as an internal standard. Coupling constants are given in Hz. Mass spectra were obtained from MALDI-TOF mass

spectrometer in Laser Desorption positive mode using α-cyano-4-hydroxycinnamic acid matrix or from High Resolution Mass Spectrometer.

The mesogenic compounds were investigated for their liquid crystalline behavior (birefringence and fluidity) by employing a polarizing optical microscope (Nikon Eclipse LV100POL) equipped with a programmable hot stage (Mettler Toledo FP90). Clean glass slides and coverslips were employed for the polarizing optical microscopic observations. The transition temperatures and associated enthalpy changes were determined by differential scanning calorimeter (Mettler Toledo DSC1) under nitrogen atmosphere. Peak temperatures obtained in DSC corresponding to transitions were in agreement with the polarizing optical microscopic observations. The transition temperatures obtained from calorimetric measurements of the first heating and cooling cycles at a rate of 5 °C/min are tabulated. In the cases where the DSC signatures are not observed for the phase transitions, the transition temperatures have been taken from microscopic observations. Temperature dependent X-ray diffraction studies were carried on unaligned powder samples in Lindemann capillaries (1 mm diameter) held in programmable hot stage and irradiated with CuKα radiation (λ = 1.5418 Å). The samples were filled in the capillary tube in their isotropic state and their both ends were flame sealed. The apparatus essentially consisted of a high-resolution powder X-ray diffractometer equipped with a focusing elliptical mirror and a high-resolution fast detector. Thermogravimetric analysis (TGA) was performed using thermogravimetric analyzer (Mettler Toledo, model TG/SDTA 851e) under constant nitrogen flow at a heating rate of 10 °C/min. UV-Vis spectra were obtained by using Perkin-Elmer Lambda 750, UV/VIS/NIR spectrometer. Fluorescence emission spectra in solution state were recorded with Horiba Fluoromax-4 fluorescence spectrophotometer or Perkin Elmer LS 50B spectrometer. Cyclic Voltammetry studies were carried out using a PAR Model 700D series Electrochemical workstation.

Conclusions

In summary, we have synthesized two series of star shaped molecules based on 1,3,4-oxadiazole and 1,3,4-thiadiazole moiety with the variation in the number and nature of the peripheral flexible chains. These two different series of molecules were synthesized through a common intermediate demonstrating the simplicity of the method. These compounds were thoroughly characterized and investigated for their thermal, photophysical and electrochemical properties. The thermal behavior was studied with the help of POM, DSC and powder XRD studies. The series based on 1,3,4-thiadiazole moiety is a new class of molecules stabilizing Col phases. We have compared this new series of molecules with their 1,3,4-oxadiazole counterparts to arrive at a structure-property correlation. 1,3,4-Thiadiazole based LCs exhibited broad mesophase range, with some of them having close to room temperature crystal to liquid crystal transitions. Many of these molecules exhibit glassy Col phase, which are beneficial for one-dimensional conductivity. The number and type of the peripheral tails have significant effect on the stabilization of liquid crystallinity of these molecules. Both the series exhibited blue luminescence in solution. Oxadiazole derivatives showed deep blue emission, while thiadiazole derivatives exhibited sky blue emission in solution state. The number and type of the peripheral tails did not have much effect on the absorption maxima, while it showed a significant shift in the emission maxima of these compounds. Thiadiazole derivatives exhibited little lower quantum yields when compared to oxadiazole derivatives. Thiadiazole derivatives are new entrants to the limited member family of blue emitting self-assembling materials. These blue emitting materials are technologically important for the fine-tuning of emission wavelength on combining with another dopant emitter in the construction of white OLEDs. Cyclic Voltammetry studies have shown that thiadiazole derivatives have a lower band gap than their

oxadiazole counterparts. These 1,3,4-thiadiazole based star shaped molecules are promising because of the ease in synthesis, stabilization of wide range hexagonal columnar phase, emission tunabilty, low band gap and thus have a potential to be used in OLEDs.

Associated Content

The synthesis and characterization details, ^{1}H NMR, ^{13}C NMR and mass spectra of all new compounds, absorption and emission spectra, POM photographs, DSC thermograms, XRD profiles of LC compounds, TGA curves and Cyclic voltammograms are provided as electronic supporting information. This material is available free of charge via the Internet at http://pubs.acs.org.

Acknowledgements

ASA sincerely thanks Science and Engineering Board (SERB), DST, Govt. of India and Board of Research in Nuclear Sciences-Department of Atomic Energy (BRNS-DAE) for funding this work through the project No.SB/S1/PC-37/2012 and No. 2012/34/31/BRNS/1039 respectively. We thank Ministry of Human Resource Development for Centre of Excellence in FAST (F. No. 5-7/2014-TS-VII). ASA acknowledges Central Instrumentation Facility, IIT Guwahati for analytical facilities. We acknowledge Dr. Chandan Mukherjee, IITGuwahati for providing his Electrochemical workstation and Dr. Santanu Kumar Pal, IISER Mohali for providing MALDI-TOF spectra.

References

(1)(a) S. Chandrasekhar, in *Liquid Crystals*, 2nd ed.; Cambridge University Press: New York, **1994**. (b) J. W. Goodby, I. M. Saez, S. J. Cowling, V. Görtz, M. Draper, A. W. Hall, S. Sia, G. Cosquer, S. –E. Lee, E. P. Raynes, *Angew. Chem. Int. Ed.* 2008, **47**, 2754-2787. (c) T. Geelhaar, K. Griesar, B. Reckmann, *Angew. Chem. Int. Ed.* 2013, **52**, 8798-8809. (d) C. Tschierske, *Angew. Chem. Int. Ed.* 2013, **52**, 8828-8878. (e) J. W. Goodby, P. J. Collings, T. Kato, C. Tschierske, H. Gleeson, P. Raynes, Eds.; *Handbook of Liquid Crystals: Fundamentals*, Wiley-VCH: Weinheim, Germany, 2014; *Vol. 1*.

(2)(a) F. Renitzer, *Monatsch. Chem.* 1888, **9**, 421-441. (b) F. Reinitzer, *Liq. Cryst.* 1989, **5**, 7–18.

(3)G. W. Gray, K. J. Harrison, J. A. Nash, *Electron. Lett.* 1973, **9**, 130-131.

(4)S. Chandasekhar, B. K. Sadashiva, K. A. Suresh, *Pramana* 1977, **9**, 471-480.

(5)(a) S. Sergeyev, W. Pisula, Y.H. Geerts, *Chem. Soc. Rev*. 2007, **36**, 1902−1929. (b) S. Laschat, A. Baro, N. Steinke, F. Giesselmann, C. Hagele, G. Scalia, R. Judele, E. Kapatsina, S. Sauer, A. Schreivogel, M. Tosoni, *Angew. Chem., Int. Ed*. 2007, **46**, 4832−4837. (c) W. Pisula, M. Zorn, J. Y. Chang, K. Müllen, R. Zentel, *Macromol. Rapid Commun.* 2009, **30**, 1179−1202. (d) S. Kumar, *Chemistry of Discotic Liquid Crystals: From Monomers to Polymers*; CRC Press: Boca Raton, FL, 2010. (e) B. R. Kaafarani, *Chem. Mater*. 2011, **23**, 378−396. (f) R. J. Bushby, K. Kawata, *Liq. Cryst*. 2011, **38**, 1415 – 1426. (g) Q. Li, *Self-Organized semiconductors: From Materials to Device Applications*; John Wiley & Sons: New York, 2011. (h) S. Kumar, *Isr. J. Chem.* 2012, **52**, 820 –

829. (i) Q. Li, *Nanoscience with Liquid Crystals: From Self-Organized Nanostructures to Applications*, Ed., Springer, Heidelberg, 2014. (j) X. Zhou, S. Kang, S. Kumar, R. Kulkar, S. Z. D. Cheng, Q. Li, *Chem. Mater.* 2008, **20**, 3551-3553. (k) X. Zhou, S. Kang, S. Kumar and Q. Li, Liq. Cryst. 2009, **3**, 269-274.

(6) K. Kawata, *Chem. Rec.* 2002, **2**, 59 – 80.

(7) S. Chandrasekhar, S. K. Prasad, G. G. Nair, D. S. S. Rao, S. Kumar, M. Manickam, *EuroDisplay-99, The 19th Intl. Display Res. Conf. Late-News Papers* 1999, 9–11.

(8) G. G. Nair, D. S. S. Rao, S. K. Prasad, S. Chandrasekhar, S. Kumar, *Mol. Cryst. Liq. Cryst.* 2003, **397**, 245 – 252.

(9) V. S. K. Balagurusamy, S. K. Prasad, S. Chandrasekhar, S. Kumar, M. Manickam, C. V. Yelamaggad, *Pramana* 1999, **53**, 3 – 11.

(10) (a) L. S. Mende, A. Fechtenkotter, K. Mullen, E. Moons, R. H. Friend, J. D. MacKenzie, *Science* 2001, **293**, 1119 – 1122. (b) H. C. Hesse, J. Weickert, M. Al-Hussein, L. Dössel, X. Feng, K. Mullen, L. S. Mende, *Solar Energy Materials & Solar Cells* 2010, **94**, 560–567. (c) Q. Sun, L. Dai, X. Zhou, L. Li, Q. Li, *Applied Physics Letters* 2007, **91**, 253505/1-253505/3.

(11) (a) A. Bacher, I. Bleyl, C. H. Erdelen, D. Haarer, W. Paulus, H. W. Schmidt, *Adv. Mater.* 1997, **9**, 1031 – 1035. (b) A. Bacher, C. H. Erdelen, W. Paulus, H. Ringsdorf, H. W. Schmidt, P. Schuhmacher, *Macromolecules,* 1999, **32**, 4551–4557. (c) I. Seguy, P. Destruel, and H. Bock, *Synthetic Metals* 2000, **111**, 15–18. (d) T. Hassheider, S. A. Benning, H. S. Kitzerow, M. F. Achard, H. Bock, *Angew Chem Int Ed.* 2001, **40**, 2060–2063. (e) S. Alibert-Fouet, S. Dardel, H. Bock, M. Oukachmih, S. Archambeau, I. Seguy, P. Jolinat, and P. Destruel, *ChemPhysChem*, 2003, **4**, 983–985. (f) M. O'Neill, S. M. Kelly, *Adv. Mater.* 2011, **23**, 566-584. (g) J. Eccher, G. C. Faria, H. Bock, H. von Seggern, I. H. Bechtold, *ACS Appl Mater Interfaces,* 2013, **5**, 11935–11943.

(12) (a) A. M. van de Craats, N. Stutzmann, O. Bunk, M. M. Nielsen, M. Watson, K. Mullen, H. D. Chanzy, H. Sirringhaus, R. H. Friend, *Adv. Mater.* 2003, **15**, 495 – 499. (b) S. Cherian, C. Donley, D. Mathine, L. LaRussa, W. Xia, N. Armstrong, *J. Appl. Phys.* 2004, **96**, 5638 – 5643. (c) B. A. Jones, M. J. Ahrens, M.-H Yoon, A. Facchetti, T. J. Marks, M. R. Wasielewski, *Angew. Chem., Int. Ed.*, 2004, **43**, 6363–6366. (d) I. O. Shklyarevskiy, P. Jonkheijm, N. Stutzmann, D. Wasserberg, H. J. Wondergem, P. C. M. Christianen, A. P. H. J. Schenning, D. M. de Leeuw, Z. Tomovic, J. Wu, K. Mullen, J. C. Maan, *J. Am. Chem. Soc.* 2005, **127**, 16233 – 16237. (e) W. Pisula, A. Menon, M. Stepputat, I. Lieberwirth, U. Kolb, A. Tracz, H. Sirringhaus, T. Pakula, K. Mullen, *Adv. Mater.* 2005, **17**, 684 – 689. (f) S. Xiao, M. Myers, Q. Miao, S. Sanaur, K. Pang, M. L. Steigerwald, C. Nuckolls, *Angew. Chem. Int. Ed.* 2005, **44**, 7390 – 7394. (g) J. Y. Cho, B. Domercq, S. C. Jones, J. Yu, X. Zhang, Z. An, M. Bishop, S. Barlow, S. R. Marder, B. J. Kippelen, *Mater. Chem*. 2007, **17**, 2642 – 2647. (h) Y. Shimizu, K. Oikawa, K. I. Nakayama, D. Guillon, *J. Mater. Chem.* 2007, **17**, 4223 – 4229. (i) H. N. Tsao, H. J. Rader, W. Pisula, A. Rouhanipour, K. Mullen, *Phys. Stat. Sol. A*. 2008, **205**, 421 – 429. (j) J. P. Bramble, D. J. Tate, D. J. Revill, K. H. Sheikh, J. R. Henderson, F. Liu, X. Zeng, G. Ungar, R. J. Bushby, S. D. Evans, *Adv. Funct. Mater.* 2010, **20**, 914–920.

(13) (a) J. D. Wright, P. Roisin, G. P. Rigby, R. J. M. Nolte, M. J. Cook, S. C. Thorpe, *Sens. Actuators B* 1993, **13**, 276 – 280. (b) J. Clements, N. Boden, T. D. Gibson, R. C. Chandler, J. N. Hulbert, E. A. Ruck-Keene, *Sens. Actuators B* 1998, **47**, 37–42. (c) N. Boden, R. J. Bushby,

J. Clements B. Movaghar *J. Mater. Chem.* 1999, **9**, 2081–2086. (d) V. Bhalla, A. Gupta, M. Kumar, D. S. S. Rao, S. K. Prasad, *ACS Appl Mater Interfaces,* 2013, **5**, 672–679.

(14) (a) D. D. L. Chung, *J. Mater. Sci.* 2002, **37**, 1475 – 1489. (b) A. Venu Gopal, P. Venkateswara Rao, *Mater. Manufact. Processes* 2004, **19**, 177 – 186. (c) K. Kawata, O. Nobuyosi, *Fujifilm Res. Dev*. 2006, **51**, 80 – 85.

(15) (a) V. V. Titov, A. I. Pavlyuchenko, *Chem. Heterocycl. Compd.* 1980, **16**, 1 – 13. (b) M. P. Aldred, P. Vlachos, D. Dong, S. P. Kitney, W. C. Tsoi, M. O. Neill, S. M. Kelly, *Liq. Cryst*. 2005, **32**, 951 – 965. (c) A. Seed, *Chem. Soc. Rev*. 2007, **36**, 2046 – 2069. (d) B. Roy, N. De, K. C. Majumdar, *Chem. Eur. J*. 2012, **18**, 14560–14588. (e) J. Han, *J. Mater. Chem. C* 2013, **1**, 7779-7797.

(16) A. C. Grimsdale, K. Leok Chan, R. E. Martin, P. G. Jokisz, A. B. Holmes, *Chem Rev*. 2009, **109**, 897–1091.

(17) (a) C. S. Wang, G. Y. Jung, Y. L. Hua, C. Pearson, M. R. Bryce, M. C. Petty, A. S. Batsanov, A. E. Goeta, J. A. K. Howard, *Chem. Mater.* 2001, **13**, 1167 – 1173. (b) A. P. Kulkarni, C. J. Tonzola, A. Babel, S.A. Jenekhe, *Chem. Mater.* 2004, **16**, 4556–4573.

(18) (a) D. Acierno, S. Concilio, A. Diodati, P. Iannelli, S. P. Piotto, P. Scarfato, P. *Liq. Cryst*. 2002, **29**, 1383 – 1392. (b) H. H. Sung, H. C. Lin, H. C. *Liq. Cryst*. 2004, **31**, 831–840. (c) R. Cristiano, F. Ely, H. Gallardo, *Liq. Cryst.* 2005, **32**, 15–25; (d) J. Han, S. S. Y. Chui, C. M. Che, *Chem. Asian J.* 2006, **1**, 814 – 825.

(19) (a) Y. D. Zhang, K. G. Jespersen, M. Kempe, J. A. Kornfield, S. Barlow, B. Kippelen, S. R. Marder, *Langmuir,* 2003, **19**, 6534 – 6536. (b) R. Cristiano, D. M. P. D. O Santos, H. Gallardo, *Liq. Cryst.* 2005, **32**, 7–14. (c) S. Varghese, N. S. S. Kumar, A. Krishna, D. S. S. Rao, S. K. Prasad, S. Das, *Adv. Funct. Mater*. 2009, **19**, 2064 – 2073. (d) C. V. Yelamaggad, A. S. Achalkumar, D. S. S. Rao, S. K. Prasad, *J. Org. Chem.* 2009, **74**, 3168 – 3171. (e) E. Westphal, I. H. Bechtold, H. Gallardo, *Macromolecules* 2010, **43**, 1319–1328. (f)D. D. Prabhu, N. S. S. Kumar, A. P. Sivadas, S. Varghese, S. Das, *J. Phys. Chem. B* 2012, **116**, 13071–13080. (g) E. Girotto, J. Eccher, A. A. Vieira, I. H. Bechtold, H. Gallardo, *Tetrahedron* 2014, **70**, 3355–3360.

(20) (a) J. Bettenhausen, P. Strohriegl, *Macromol. Rapid Commun.* 1996, **17**, 623 – 631. (b) T. Christ, B. Glüsen, A. Greiner, A. Kettner, R. Sander, V. Stümpflen, V. Tsukruk, J. H. Wendorff, *Adv. Mater*. 1997, **9**, 219-222. (c) J. Bettenhausen, M. Greczmiel, M. Jandke, P. Strohriegl, *Synth. Met.* 1997, **91**, 223–228. (d) A. C. Sentman, D. L. Gin, *Adv. Mater.* 2001, **13**, 1398–1401. (e) B. G. Kim, S. Kim, S. Y. Park, *Tetrahedron Lett.* 2001, **42**, 2697 – 2699. (f) C. K. Lai, Y.-C. Ke, J.–C. Su, C. Shen, W. –R. Li, *Liq. Cryst.* 2002, **29**, 915–920. (g) B. G. Kim, S. Kim, J. Seo, N.–K. Oh, W.–C. Zin, S. Y. Park, *Chem. Commun.* 2003, 2306–2307. (h) S. Qu, M. Li, *Tetrahedron* 2007, **63**, 12429–12436. (i) J. Seo, S. Kim, S. H. Gihm, C. R. Park, S. Y. Park, *J. Mater. Chem.* 2007, *17*, 5052–5057. (j) H. Wang, F. Zhang, B. Bai, P. Zhang, J. Shi, D. Yu, Y. Zhao, Y. Wang, M. Li, *Liq. Cryst*. 2008, **35**, 905 – 912. (k) J. Tang, R. Huang, H. Gao, X. Cheng, M. Prehm, C. Tschierske, *RSC Adv*. 2012, **2**, 2842 – 2847. (l) E. Westphal, M. Prehm, I. H. Bechtold, *J. Mater. Chem. C* 2013, **1**, 8011–8022.

(21) (a) P. J. Martin D. W. Bruce, *Liq. Cryst.* 2007, **34**, 767–774. (b) A. A. Vieira, H. Gallardo, J. Barbera, P. Romero, J. L. Serrano, T. Sierra, *Mater. Chem.* 2011, **21**, 5916 – 5922. (c) J. Han, Q. Geng, W. Chen, L. Zhu, Q. Wu, Q. Wang, *Supramol. Chem*. 2012, **24**, 157–164.

(22) (a) D. Haristoy D. Tsiourvas, *Chem. Mater.* 2003, **15**, 2079–2083. (b) E. Westphal, D. H. D. Silva, F. Molin, H. Gallardo, H. *RSC Adv.* 2013, **3**, 6442-6454.

(23) (a) P. I. C. Teixeira, A. J. Masters, B. M. Mulder, *Mol. Cryst. Liq. Cryst.* 1998, **323**, 167–189. (b) C. F. He, G. T. Richards, S. M. Kelly, A. E. A. Contoret, M. O'Neil, *Liq. Cryst.* 2007, **34**, 1249-1267. (c) M. L. Parra, E. Y. Elgueta, V. Jimenez, P. I. Hidalgo, *Liq. Cryst*. 2009, **36**, 301-317. (d) L.-R. Zhu, F. Yao, J. Han, J. M.-L. Pang, J.-B. Meng, *Liq. Cryst*. 2009, **36**, 209-213. (e) T. J. Dingemans, L. A. Madsen, O. Francescangeli, F. Vita, D. J. Photinos, C.-D. Poon, E. T. Samulski, *Liq. Cryst.* 2013, **40**, 1655–1677.

(24) (a) J. Han, M. Zhang, F. Wang, Q. Geng, *Liq. Cryst.* 2010, **37**, 1471–1478. (b) K. C. Majumdar, P. K. Shyam, D. S. S. Rao, S. K. Prasad, *J. Mater. Chem.*, 2011, **21**, 556-561.

(25) (a) P. E. Cassidy, N. C. Fawcett, *J. Macromol. Sci. Rev. Macromol. Chem. Phys.* 1979, **C17**, 209–266. (b) X. C. Li, A. Kraft, R. Cervini, G. C. W. Spencer, F. Cacialli, R. H. Friend, J. Gruener, A. B. Holmes, J. C. DeMello, S. C. Moratti, *Mater. Res. Soc. Symp. Proc.* 1996, **413**, 13–22. (c) H. H. Sung, H. C. Lin, *Macromolecules*, 2004, **37**, 7945 – 7954. (d) M. Sato, Y. Tada, S. Nakashima, K. I. Ishikura, M. Handa, K. Kasuga, *J. Polym. Sci. Part A Polym.Chem.* 2005, **43**, 1511 – 1525. (e) M. Sato, Y. Matsuoka, I. Yamaguchi, *J. Polym. Sci. Part A Polym. Chem.* 2007, **45**, 2998 – 3008.

(26) J. Han, X. Y. Chang, L. R. Zhu, M.-L. Pang, J. B. Meng, S. S.-Y. Chui, S. W. Lai, V. A. L. Roy, *Chem Asian J* 2009, **4**, 1099–1107.

(27) Y. Hu, C.-Y. Li, X.-M. Wang, Y.-H. Yang, H.-L. Zhu, *Chem Rev,* 2014, **114**, 5572–5610.

(28) D. Adam, P. Schuhmacher, J. Simmerer, L. Hayssling, K. Siemensmeyer, K. H. Etzbach, H. Ringsdorf, D. Haarer, *Nature* 1994, **371**, 141-143.

(29) (a) M. Parra, S. Hernandez, J. Alderete, C. Zuniga, *Liq. Cryst*. 2000, **27**, 8, 995-1000. (b) Y. Xu, W. Lu, Z. Tai, *Molecular Crystals and Liquid Crystals Science and Technology. Section A. Molecular Crystals and Liquid Crystals* 2000, **350**, 151–159. (c) A. A. Kiryanov, P. Sampson, A. J. Seed, *J. Org. Chem.* 2001, **66**, 7925-7929. (d) M. W. Schroder, S. Diele, G. Pelzl, N. Pancenko, W. Weissflog, *Liq. Cryst.* 2002, **29**, 1039 – 1046. (e) M. Parra, J. Alderete, C. Zuniga, *Liq. Cryst.* 2004, **31**, 1531–1537. (f) T. Hegmann, B. Neumann, R. Wolf, C. Tschierske, *J. Mater. Chem.* 2005, **15**, 1025–1034. (g) M. Parra, J. Vergara, P. Hidalgo, J. Barbera, T. Sierra, *Liq. Cryst.* 2006, **33**, 739 – 745. (h) B. P. Sybo, A. Bradley, S. Grubb, K. Miller, J. W. Proctor, L. Clowes, M. R. Lawrie, P. Sampson, A. J. Seed, *J. Mater. Chem*. 2007, **17**, 3406 – 3411. (i) C. F. He, G. J. Richards, S. M. Kelly, A. E. A. Contoret, M. O. Neill, *Liq. Cryst*. 2007, **34**, 1249 – 1267. (j) J. Han, X. Y. Chang, L. R. Zhu, Y. M. Wang, J. B. Meng, S. W. Lai, S. S.-Y. Chui, *Liq. Cryst*. 2008, **35**, 1379–1394. (k) J. H. Tomma, I. H. Rou'il, A. H. Al-Dujaili, *Mol. Cryst. Liq. Cryst*. 2009, **501**, 3–19. (l) M. C. McCairn, T. Kreouzis, M. L. Turner, *J. Mater. Chem.* 2010, **20**, 1999-2006. (m) A. K. Prajapati, V. Modi, *Liq. Cryst*. 2011, **38**, 191–199. (n) Q. Song, D. Nonnenmacher, F. Giesselmann, R. P. Lemieux, *J. Mater. Chem. C*, 2012, **1**, 343-350. (o) P. Tuzimoto, D. M. P. O. Santos, T. D. S. Moreira, R. Cristiano, I. H. Bechtold, H. Gallardo, *Liq. Cryst.* 2014, **41**, 1097–1108. (p) R. C. Tandel N. K. Patel, *Liq. Cryst.* 2014, **41**, 495–502.

(30) (a) M. Lehmann, J. Seltmann, A. Auer, E. Prochnow, U. Benedikt, U. *J. Mater. Chem.* 2009, **19**, 1978–1988. (b) M. Lehmann, J. Seltmann, *Beilstein J. Org. Chem*. 2009, **5**, 73 (1-9).

(31) M. L. Parra, E. Y. Elgueta, J. A. Ulloa, J. M. Vergara, A. I. Sanchez, *Liq. Cryst.* 2012, **39**, 917–925.

(32) (a) M. Sato, *Macromol Rapid Commun*. 1999, **20**, 77–80. (b) M. Sato, Y. Uemoto, *Macromol. Rapid Commun.* 2000, **21**, 1220-1225. (c) M. Sato, M. Notsu, S. Nakashima, Y. Uemoto, *Macromol. Rapid Commun.* 2001, **22**, *No. 9*, 681–686. (d) M. Sato, M. Mizoi, Y. Uemoto,

Macromol. Chem. Phys. 2001, **202**, 3634–3641. (e) M. Sato, S. Nakashima, Y. Uemoto, *J. Polym. Sci. A Polym. Chem*, 2003, **41**, 2676 –2687. (f) N. S. Al-Muaikel, *Polym Int*, 2004, **53**, 301–306. (g) M. Sato, Y. Tada, S. Nakashima, K.-I. Ishikura, M. Handa, K. Kasuga, *J. Polym. Sci. A Polym. Chem.*, 2005, **43**, 1511–1525. (h) M. Sato, Y. Matsuoka, I. Yamaguchi, *Liq. Cryst.* 2012, **39**, 1071–1081.

(33) (a) M. Parra, S. Villouta, V. Vera, J. Belmar, C. Zuniga, H. Z. Zunza, *Naturforsch. B* 1997, **52**, 1533–1538. (b) M. Sato, R. Ishii, S. Nakashima, K. Yonetake, J. Kido, *Liq. Cryst.* 2001, **28**, 1211 – 1214. (c) C. F. He, G. J. Richards, S. M. Kelly, A. E. A. Contoret, M. O'Neill, *Liq. Cryst.*, 2007, **34**, 1249–1267. (d) J. H. Tomma, I. H. Rou'il, A. H. Al-Dujaili, *Mol. Cryst. Liq. Cryst.* 2009, **501**, 3–19.

(34) (a) K.-T. Lin, H.-M. Kuo, H.-S. Sheu, C. K. Lai, *Tetrahedron* 2013, **69**, 9045-9055. (b) K. S. Mustafa, K. S. Al-Malki, A. S. Hameed, A. H. Al-Dujaili, *Mol. Cryst. Liq. Cryst.* 2014, **593**, 34–42.

(35) (a) A. S. Achalkumar, U. S. Hiremath, D. S. Shankar Rao, S. Krishna Prasad, C. V. Yelamaggad, *J. Org. Chem.* 2013, **78**, 527−544. (b) I. Thomsen, K. Clausen, S. Scheibye, S.-O. Lawesson, *Organic Syntheses* 1990*,* **7***,* 372-373.

(36) S. Chandrasekhar, In *Advances in Liquid Crystals*; Brown, G. H., Ed.; Academic Press: New York, 1982; **Vol. 5**, p 47.

(37) (a) C. Carfagna, A. Roviello, A. Sirigu, *Mol. Cryst. Liq. Cryst.* 1985, **122**, 151−160. (b) E. F. Gramsbergen, H. J. Hoving, W. H. de Jeu, K. Praefcke, B. Kohne, *Liq. Cryst.* 1986, **1**, 397−400. (c) H. Metersdorf, H. Ringsdorf, *Liq. Cryst.* 1989, **5**, 1757−1772. (d) H. Zeng, P. J. Carroll, T. M. Swager, *Liq. Cryst*. 1993, **14**, 1421− 1429. (e) C. F. Van Nostrum, A. W. Bosman, G. H. Gelinck, P. G. Schouten, J. M. Warman, A. P. M. Kentgens, M. A. C. Devillers, A. Meijerink, S. J. Picken, U. Sohling, A.-J. Schouten, R. J. M. Nolte, *Chem. Eur. J.* 1995, **1**, 171−182. (f) J. Barbera, R. Gimenez, J. L. Serrano, *Chem. Mater*. 2000, **12**, 481−489. (g) J. L. Serrano, T. Sierra, *Chem. Eur. J*. 2000, **6**, 759−766. (h) S. Ito, M. Ando, A. Nomura, N. Morita, C. Kabuto, H. Mukai, K. Ohta, J. Kawakami, A. Yoshizawa, A. Tajiri, *J. Org. Chem.* 2005, **70**, 3939−3949. (i) A. Hayer, V. de Halleux, A. Kohler, A. El-Garoughy, E. W. Meijer, J. Barbera, J. Tant, J. Levin, M. Lehmann, J. Gierschner, J. Cornil, Y. H. Geerts, *J. Phys. Chem. B* 2006, **110**, 7653−7659. (j) L. Alavarez, J. Barbera, L. Puig, P. Romero, J. L. Serrano, T. Sierra, *J. Mater. Chem.* 2006, **16**, 3768−3773. (k) C. V. Yelamaggad, A. S. Achalkumar, D. S. S. Rao, S. K. Prasad, *J. Mater. Chem.* 2007, **17**, 4521−4529. (l) C. V. Yelamaggad, A. S. Achalkumar, D. S. S. Rao, S. K. Prasad, *J. Org. Chem.* 2007, **72**, 8308−8318. (m) C. V. Yelamaggad, A. S. Achalkumar, D. S. S. Rao, M. Nobusawa, H. Akutsu, J. Yamada, S. Nakatsuji, *J. Mater. Chem.* 2008, **18**, 3433−3437.

(38) V. Percec, M. Glodde, T. K. Bera, Y. Miura, I. Shiyanovskaya, K. D. Singer, V. S. K. Balagurusamy, P. A. Heiney, I. Schnell, A. Rapp, H.-W. Spiess, S. D. Hudsonk, H. Duank, *Nature* 2002, **419**, 384-387.

(39) (a) D. M. Collard, C. P. Lillya, *J. Am. Chem. Soc.* 1987, **109**, 7544-7545. (b) R. Festag, R. Kleppinger, M. Soliman, J. H. Wendorff, G. Lattermann, G. Staufer, *Liq. Cryst*. 1992, **11**, 699-710. (c) R. Kleppinger, C. P. Lillya, C. Yang, *J. Am. Chem. Soc.* 1997, **119**, 4097-4102. (d) C. V. Yelamaggad, A. S. Achalkumar, *Tetrahedron Lett.* 2012, **53**, 7108-7112.

(40) (a) C. Adachi, T. Tsutui, S. Saito, *Appl. Phys. Lett.* 1990, **56**, 799-801. (b) H. Antoniadis, M. Inbasekaran, E. P. Woo, *Appl. Phys. Lett.* 1998, **73**, 3055-3057. (c) N. –X. Hu, M. Esteghamatian, S. Xie, Z. Popovic, Ah.-M. Hor, O. Beng, S. Wang, S. *Adv. Mater.* 1999, **11**,

1460–1463. (d) S. Tao, Z. Peng, P. Wang, C. –S. Lee, S. –T. Lee, *Adv. Funct. Mater.* 2005, **15**, 1716–721.

(41) (a) Y. Li, Y. Cao, J. Gao, D. Wang, G. Yu, A. J. Heeger, *Synth. Met*. 1999, **99**, 243–248. (b) L. Dou, J. You, J. Yang, C.–C. Chen, Y. He, S. Murase, T. Moriarty, K. Emery, G. Li, Y. Yang, *Nat. Photonics* 2012, **6**, 180–185. (c) P. Deng, L. Liu, S. Ren, H. Li, Q. Zhang, *Chem. Commun.* 2012, **48**, 6960–6962. (d) C. V. Yelamaggad, A.S. Achalkumar, D. S. Shankar Rao, S. K. Prasad, *Org. Lett.* 2007, **9**, 2641–264.

Dr. A. S. Achalkumar
Assistant Professor
Department of Chemistry
Indian Institute of Technology Guwahati
Guwahati – 781039, Assam, India
Phone: +91-361-258-2329
Fax: +91-361-258-2349
E-mail: achalkumar@iitg.ernet.in
achalkumar78@gmail.com

Table of Contents Graphic

Blue Light Emitting Star shaped Oxadiazole and Thiadiazoles Stabilizing Fluid Columnar phase